© 2014. Published by The Company of Biologists Ltd | Journal of Cell Science (2014) 127, 4429–4442 doi:10.1242/jcs.151738

RESEARCH ARTICLE

The meiosis-specific nuclear passenger protein is required for proper assembly of forespore membrane in fission yeast

Masak Takaine[1,*], Kazuki Imada[2], Osamu Numata[1], Taro Nakamura[2] and Kentaro Nakano[1,*]

ABSTRACT

Sporulation, gametogenesis in yeast, consists of meiotic nuclear division and spore morphogenesis. In the fission yeast *Schizosaccharomyces pombe*, the four haploid nuclei produced after meiosis II are encapsulated by the forespore membrane (FSM), which is newly synthesized from spindle pole bodies (SPBs) in the cytoplasm of the mother cell as spore precursors. Although the coordination between meiosis and FSM assembly is vital for proper sporulation, the underlying mechanism remains unclear. In the present study, we identified a new meiosis-specific protein Npg1, and found that it was involved in the efficient formation of spores and spore viability. The accumulation and organization of the FSM was compromised in *npg1*-null cells, leading to the error-prone envelopment of nuclei. Npg1 was first seen as internuclear dots and translocated to the SPBs before the FSM assembled. Genetic analysis revealed that Npg1 worked in conjunction with the FSM proteins Spo3 and Meu14. These results suggest a possible signaling link from the nucleus to the meiotic SPBs in order to associate the onset of FSM assembly with meiosis II, which ensures the successful partitioning of gametic nuclei.

KEY WORDS: Meiosis, Sporulation, Forespore membrane, Fission yeast, Spindle pole body

INTRODUCTION

Gametogenesis is essential for sexual reproduction and consists of meiosis and the specialized development of haploid cells. Ascospore formation in the fission yeast *Schizosaccharomyces pombe* fundamentally corresponds to the formation of gametes in other organisms, but is unique in that haploid daughter cells are newly synthesized in the cytoplasm of the mother cell without cell division. The sporulation of yeasts has been intensively studied for many years, leading to an overall picture of the dynamical and multistep differentiation process phenomenologically as well as at the molecular level (reviewed in Shimoda, 2004; Neiman, 2011). Briefly, under nitrogen starvation conditions, *S. pombe* haploid cells arrest their cell cycles in G1 and start to conjugate to the neighbors of opposite mating types to produce diploid zygotes following nuclear fusion. After premeiotic DNA synthesis, the nucleus elongates and oscillates for approximately 2 h, a process which is termed horsetail movement and has been implicated in the efficient pairing and recombination of homologous chromosomes (Hiraoka, 1998). Two consecutive meiotic nuclear divisions generate four prespores, each of which contains one haploid nucleus and a set of organelles and is wrapped by a double-layered membrane called the forespore membrane (FSM) (the prospore membrane in budding yeast). These prespores are gradually covered by the spore wall and mature to long-living spores that exhibit strong resistance to environmental insults.

The most interesting part of yeast sporulation is the assembly of the FSM. To ensure the distribution of four haploid genomes to each prespore, a second meiotic nuclear division and the enfoldment of nuclei by the FSM must be accurately coordinated in both space and time. SPBs in yeast are functional equivalents of the centrosome in mammalian cells, which organizes microtubules for the assembly of mitotic spindles. SPBs also play an essential role in the coordinated formation of the FSM. After meiosis I, SPBs embedded in the nuclear envelope are duplicated, and a multilayered plaque, which is called the meiotic outer plaque, then emerges at the cytoplasmic side of the SPBs at prophase II. The formation of this plaque was originally observed using electron microscopy (Tanaka and Hirata, 1982) and has also been detected with a fluorescence microscope as a change in the appearance of the SPB signal from a dot to a crescent form (Hagan and Yanagida, 1995). These morphological alternations in SPBs are collectively referred to as SPB modifications and are crucial for sporulation (Ikemoto et al., 2000). Membrane vesicles are targeted on the outer sides of the plaque and fuse into arc-shaped nascent FSM by metaphase II. During anaphase II, two FSM sacs expand from the poles encasing a nucleus, and the nucleus elongates with the intranuclear spindle to divide into two, and these sacs finally enclose two newborn nuclei individually. The leading edge of the elongating FSM forms a ring and comprises some associated proteins. The enclosure of the FSM sac has been implicated in the constriction of the leading edge ring (Okuzaki et al., 2003).

Many sporulation-related genes (spo^+) in *S. pombe* have been identified and characterized (Shimoda, 2004). The coiled-coil protein Spo15 has been shown to constitutively localize to the SPBs depending on the function of the calmodulin Cam1 (Itadani et al., 2010) and is essential for SPB modifications (Ikemoto et al., 2000). A previous study has reported that Spo2 and Spo13 are sequentially recruited to meiotic SPBs and form a complex with Spo15 to complete this modification (Nakase et al., 2008). The syntaxin (mammalian t-SNARE protein)-related protein Psy1 and meiosis-specific coiled-coil protein Spo3 have been shown to assemble the FSM precursor and initiate its expansion (Nakamura et al., 2001). Spo14 and Spo20 are the homologs of the *S. cerevisiae* Sec proteins (secretary pathway components) Sec12 and Sec14, respectively, and have been shown to play a role in the development of the FSM (Nakase et al., 2001; Nakamura-Kubo

[1]Department of Biological Sciences, Graduate School of Life and Environmental Sciences, University of Tsukuba, 1-1-1 Tennohdai, Tsukuba, Ibaraki 305-8577, Japan. [2]Department of Biology, Graduate School of Science, Osaka City University, Sumiyoshi-ku, Osaka 558-8585, Japan.

*Authors for correspondence (masaktakaine@gmail.com; knakano@biol.tsukuba.ac.jp)

Received 17 February 2014; Accepted 5 August 2014

Journal of Cell Science

Journal of Cell Science (2014) 127, 4429–4442 doi:10.1242/jcs.151738

et al., 2003), which suggests that membrane vesicle fusion is fundamental to extension of the FSM. Septins localize partially to the developing FSM and might orient membrane expansion (Onishi et al., 2010). Meu14, the only identified leading edge protein in fission yeast, is known to localize to the leading edge rings and is essential for proper sporulation (Okuzaki et al., 2003). F-actin also assembles into broader rings at the leading edges and might stabilize them (Petersen et al., 1998; Itadani et al., 2006; Yan and Balasubramanian, 2012). The pleckstrin homology domain protein Spo7 localizes to the SPBs after meiosis I, and should harmonize the launch of the FSM and organization of the leading edge because it can interact directly with Meu14 (Nakamura-Kubo et al., 2011). Recent studies have demonstrated that the septation initiation network (SIN) is also involved in the formation of spores. The activity of the SIN comprises three protein kinases (Sid1, Sid2, and Cdc7) that localize to the SPBs and are required for cytokinesis, septum formation and their coordination (reviewed in Goyal et al., 2011). SIN components also localize to the meiotic SPBs and have been implicated in the assembly of the FSM (Krapp et al., 2006). The meiosis-specific Sid2-related kinase Slk1/Mug27 has been shown to cooperate with Sid2 in order to develop the FSM (Ohtaka et al., 2008; Pérez-Hidalgo et al., 2008; Yan et al., 2008). Previous studies have reported that Dma1, a negative regulator of the SIN (Murone and Simanis, 1996), also localized to the meiotic SPBs and regulates the assembly of the FSM in parallel with Meu14, septins and Slk1/Mug27 (Krapp et al., 2010; Li et al., 2010).

Meiotic nuclear division and FSM assembly must be properly ordered for the successful formation of prespores. Despite the numerous aforementioned studies, the signaling pathway to strictly trigger the assembly of the FSM at prophase II remains elusive. We here demonstrate that the meiosis-specific protein Npg1 is involved in the accumulation and organization of the FSM and is, hence, required for proper sporulation. Moreover, Npg1 initially appeared in the nucleus post meiosis I, and then moved to the SPBs shortly before the onset of FSM assembly. Our results suggest that Npg1 might ensure that the start of the FSM expansion program is coupled to the timing of meiotic

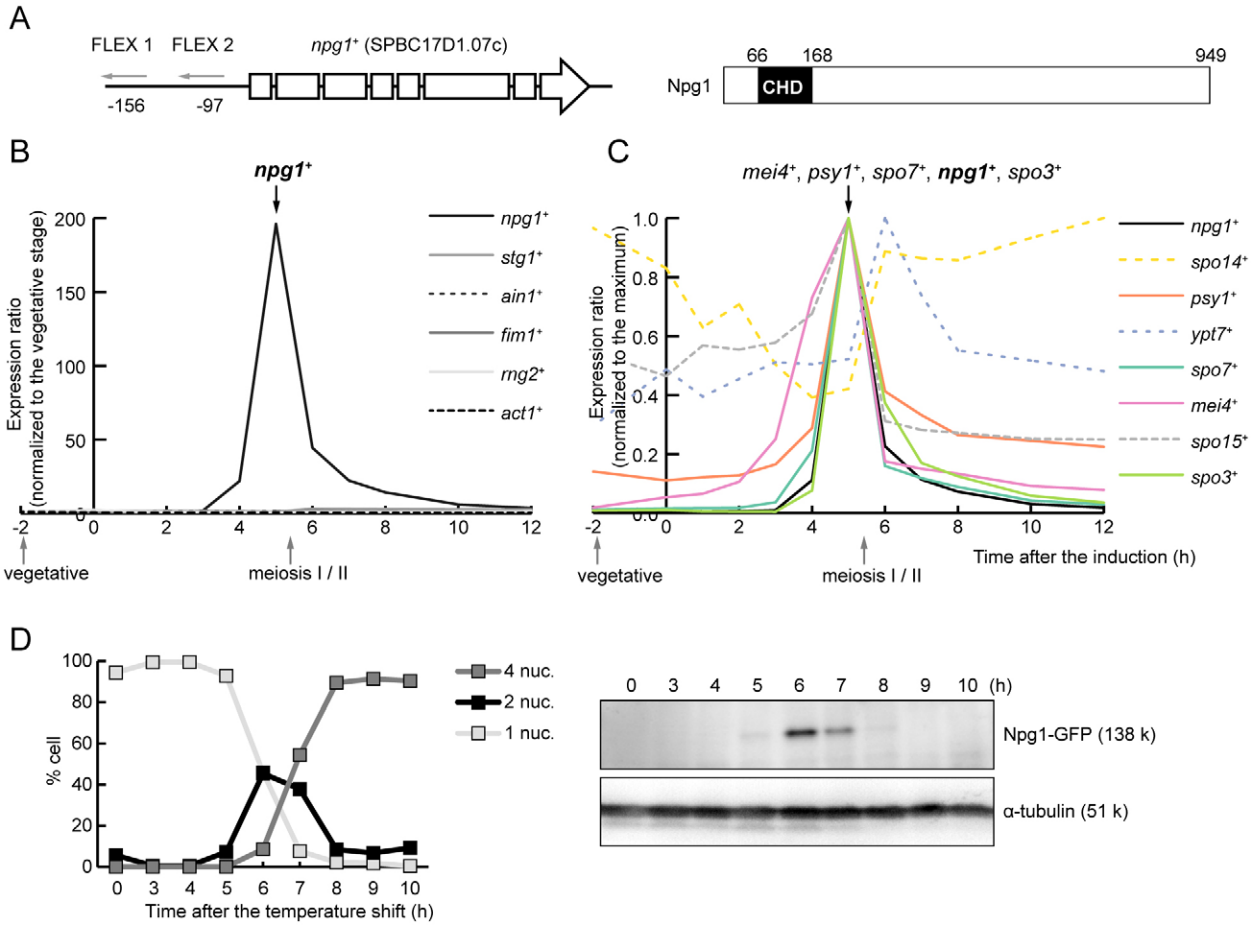

Fig. 1. Expression of the Npg1 gene. (A) Schematic diagram of Npg1. The *npg1*$^+$ gene consists of eight exons. Two FLEX-like consensus sequences (GTAAACA) are in the promoter region. (B) *npg1*$^+$ is the sole CHD-family gene whose expression is upregulated in meiosis. The expression profiles of actin (*act1*$^+$) and the five fission yeast genes containing CHD during meiosis are shown. Data were downloaded from the Gene Expression Viewer (http://128.40.79.33/cgi-bin/SPGE_/geexview). The *x*-axis indicates the time after the thermal inactivation of Pat1 kinase, which induces synchronized meiosis. The expression level of each gene was normalized to that in vegetative cells. Stg1 is an SM22/transgelin-like protein; Ain1 is an α-actinin; Fim1 is a fimbrin; Rng2 is an IQGAP-like protein required for cytokinesis. (C) The expression profile of *npg1*$^+$ is similar to those of some genes essential for sporulation. The expression profiles of *npg1*$^+$ were aligned with those of several genes required for prespore formation. Each profile was normalized to the maximum expression level of the gene. (D) Western blot analysis of the protein level of Npg1 during meiosis. *pat1-114 npg1-GFP* cells were subjected to synchronous meiosis by shifting the temperature from 25℃ to 34℃ and were sampled at each time point. Meiotic nuclear division was monitored by counting the number of nuclei per cell. Npg1–GFP was detected as a 138-kDa band. The levels of α-tubulin are shown as a loading control.

Journal of Cell Science (2014) 127, 4429–4442 doi:10.1242/jcs.151738

nuclear division to ensure the efficient compartmentalization of haploid nuclei.

RESULTS

Identification of a meiosis-specific calponin homology domain protein in fission yeast

During the course of studying actin-binding proteins in *S. pombe*, we identified a gene (SPBC17D1.07c) that encoded a basic protein (a deduced pI is 9.52) with a calponin-homology domain (CHD), an actin-binding module identified in various proteins (Gimona et al., 2002), in the genome database (Fig. 1A). Although the CHD shared sequence similarities with Rng2 (~40% identical), the fission yeast IQGAP required for cytokinesis (Eng et al., 1998), other known domains, including those characteristic to IQGAP proteins [such as IQ motifs or GTPase-activating protein (GAP)-related domains], were not conserved. We demonstrated that this gene was essential for proper sporulation and named it *npg1*$^{+}$ after nuclear passenger protein 1, based on its characteristic translocalization (see below). We identified two FLEX-like elements in the 5′ upstream region. These elements have been shown to be target sequences of the meiosis-specific forkhead transcription factor Mei4, which regulates the expression of various genes essential for meiosis or sporulation (Horie et al., 1998). A comprehensive microarray expression study (Mata et al., 2002) has previously reported that the expression of *npg1*$^{+}$ mRNA is also significantly upregulated during synchronous meiosis, whereas the expression levels of four other genes encoding CHD family proteins remain constant (Fig. 1B). Genes essential for sporulation are also upregulated during meiosis, and several of them, such as *mei4*$^{+}$, *psy1*$^{+}$, *spo7*$^{+}$, and *spo3*$^{+}$, have similar expression profiles to that of *npg1*$^{+}$, which indicated the possible co-regulation of these genes (Fig. 1C). Correspondingly, the expression levels of *psy1*$^{+}$, *spo7*$^{+}$, *spo3*$^{+}$, *and npg1*$^{+}$ were previously shown to be reduced in *mei4Δ* cells and increased in Mei4-overexpressing cells (Mata et al., 2007).

We examined the expression of *npg1*$^{+}$ at the protein level during meiosis using immunoblot analysis with an Npg1–GFP strain, which expresses Npg1 tagged by the fusion of sequences encoding GFP to the native molecule at the endogenous locus. Cells bearing both *npg1-GFP* and the *pat1-114* thermosensitive mutation were induced to enter synchronous meiosis at 34℃ and

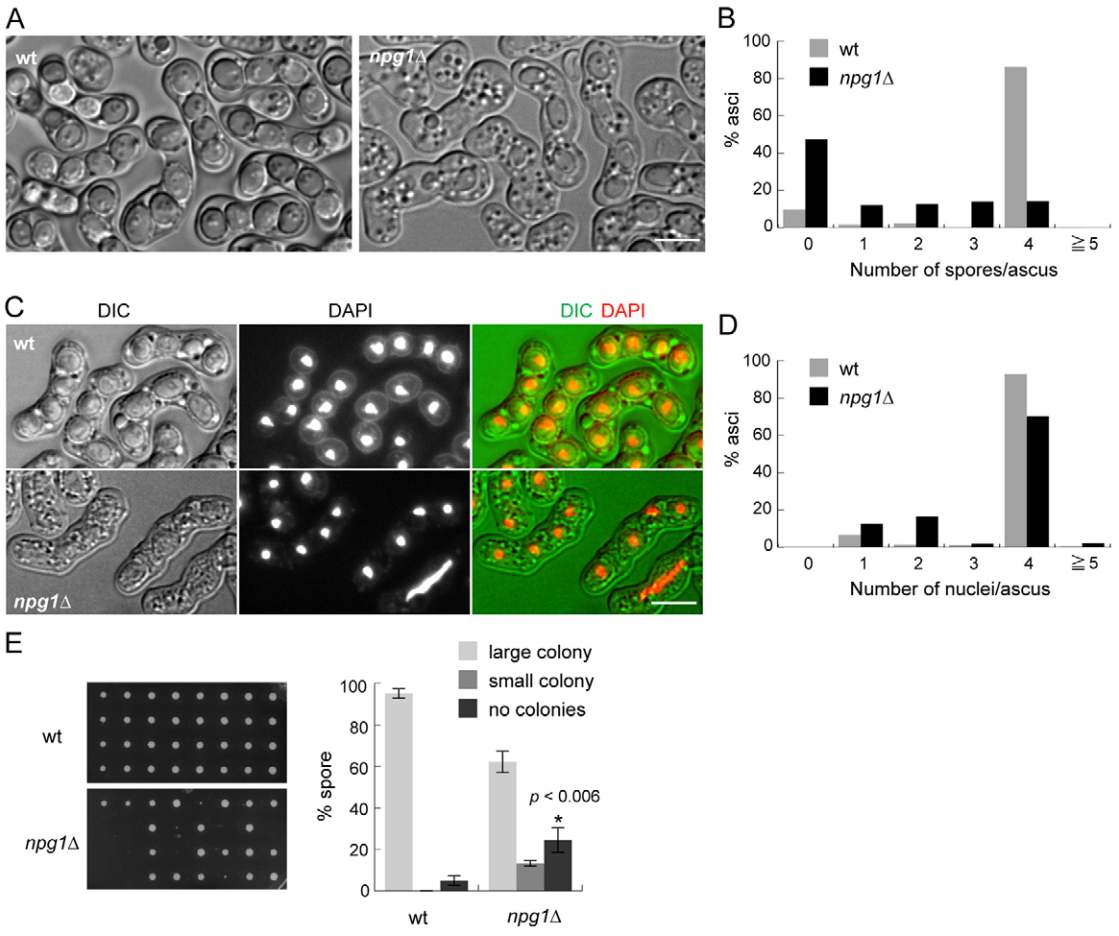

Fig. 2. Npg1 is involved in efficient sporulation and spore viability. (A) Defective sporulation in *npg1Δ* cells. Homothallic wt and *npg1Δ* cells were grown to mid-log phase and then incubated on an ME plate at 25℃ for 2 days. (B) Quantification of the number of spores per ascus. More than 500 asci from two independent preparations were scored. (C) Meiosis occurred almost normally in *npg1*Δ cells. Two-day-old asci were fixed and stained with DAPI. (D) Quantification of the number of nuclei per ascus. More than 330 asci from two independent preparations were scored. (E) Germination efficiency of wt and *npg1Δ* spores. Spores released from 4- or 5 day-old asci were randomly chosen and separated on a YE plate. The colonies formed were imaged after 4 days at 30℃. The numbers and sizes of colonies were scored. Data are the mean±s.d. from three independent preparations. More than 120 spores were examined for each preparation. *P<0.006 (Student's t-test). Scale bars: 5 µm.

Journal of Cell Science (2014) 127, 4429–4442 doi:10.1242/jcs.151738

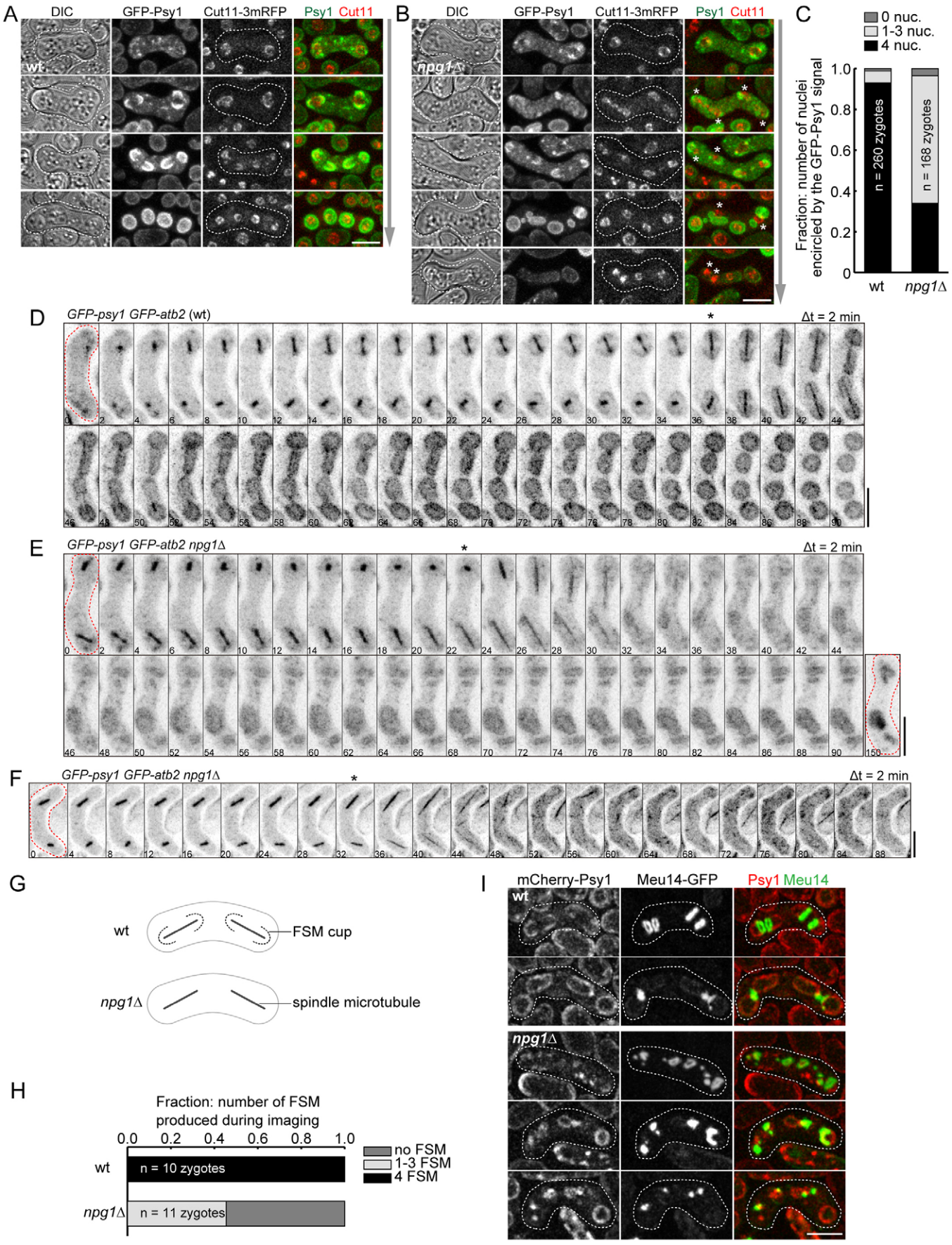

Fig. 3. See next page for legend.

Fig. 3. Npg1 is essential for the proper assembly of FSM.
(A,B) Formation of the FSM in *npg1Δ* cells. Homothallic wt (A) and *npg1Δ* (B) cells expressing GFP–Psy1 and Cut11–3mRFP were induced to undergo meiosis on ME plates at 25℃ for 12–14 h before imaging. Arrows indicate the progression of the meiotic stages. Asterisks indicate nuclei not encapsulated by the FSM. (C) Inefficient wrapping of postmeiotic nuclei by the FSM in *npg1Δ* cells. The number of nuclei encircled by GFP–Psy1 signals in cells after successful meiotic nuclear division were counted and categorized. More than 300 zygotes having four postmeiotic nuclei were prepared from two independent experiments and scored. (D–F) Time-lapse analysis of the formation of the FSM. Homothallic wt (D) and *npg1Δ* (E,F) cells expressing both GFP–Psy1 and GFP–Atb2 (labeling tubulin) were induced to enter meiosis at 25℃ for 12–14 h, and then imaged. Asterisks indicate the onset of anaphase II, during which spindles began to further elongate. (G) Schematic representation showing localization of the FSM and spindles in wt and *npg1Δ* cells at anaphase II. Cup-like structures of the FSM around the ends of spindles were hardly detectable in the mutant. (H) Quantification of FSM spheres in wt and *npg1Δ* asci. The number of spherical signals of GFP–Psy1 formed during time-lapse imaging, as shown in D–F, was counted. Data were pooled from two independent experiments. (I) Simultaneous observation of the FSM and leading edge. Homothallic wt and *npg1Δ* cells expressing both Meu14–GFP and mCherry–Psy1 were induced to enter meiosis. Cells were imaged at a single time-point, and the *z*-stacked images were deconvolved. Scale bars: 5 μm.

were occasionally sampled (Fig. 1D). Npg1–GFP was only detected 5–7 h after the induction, a time during which cells completed the first nuclear division. Thus, Npg1 was transiently produced between meiosis I and II.

Npg1 plays a role in proper sporulation and spore viability

Given that Npg1 was found to be expressed exclusively in meiosis, we next determined whether meiosis or sporulation was affected in *npg1Δ* cells. Homothallic cells were subjected to nitrogen-starvation conditions to induce mating, followed by meiosis and sporulation. More than 90% of wild-type (wt) asci contained four spores (Fig. 2A,B). In contrast, only ~10% of asci from *npg1Δ* cells contained four spores, 40% contained 1–3 spores, and the remainder (~50%) contained no spores. Despite this abnormality in sporulation, *npg1Δ* asci did not produce five or more spores. Based on the lower contrast of their contours, the walls of *npg1Δ* spores sometimes appeared to be thinner than those of wt spores. These results indicated the incomplete formation of spores in *npg1Δ* asci. Approximately 90% of wt asci contained four condensed nuclei, which correspond to the successful completion of meiosis (Fig. 2C,D). Meiotic nuclear divisions were slightly delayed in *npg1Δ* asci: 70% contained four nuclei and 16% contained two nuclei.

We assessed the viability of spores from *npg1Δ* asci. Normal-looking spores liberated from asci were randomly chosen and grown. Whereas 95% of wt spores formed colonies that were similar in size, 62% of *npg1Δ* spores formed colonies roughly the same size as those from wt spores and 13% formed smaller colonies (Fig. 2E). The fraction of *npg1Δ* spores that did not form colonies was significantly larger than that of wt spores (5% versus 24%). Therefore, germination efficiency was partially compromised in the spores produced in *npg1*Δ cells.

Npg1 is essential for proper assembly of the FSM and its coordination between meiosis II

The synthesis of the spore wall is preceded by prespore formation, in which the FSM encapsulates each of the divided four nuclei. The meiotic expression of Npg1 suggested that the role of Npg1 could be in prespore formation. Thus, we next examined the formation of prespores in *npg1Δ* zygotes. We simultaneously observed the localization of GFP–Psy1 and Cut11–3mRFP, which labels the FSM (Nakamura et al., 2001) and the nuclear envelope including SPBs, respectively. In wt zygotes, the FSM formation was initiated at prophase II, when the FSM accumulated around SPBs, and it formed cup-like structures during metaphase II (Fig. 3A). At anaphase II, during which nuclei elongate to divide, the FSM cups expanded, wrapped around these nuclei, and eventually formed four spherical prespores. The FSM also accumulated around SPBs at prophase II in *npg1Δ* zygotes; however, its local quantity was smaller than that of wt (Fig. 3B). The FSM rarely developed into proper cup-like structures and often formed aggregates or bleb-like structures, leading to the inefficient wrapping of divided nuclei (Fig. 3B, asterisks; Fig. 3C).

We conducted time-lapse imaging to further investigate how the FSM developed in *npg1Δ* cells. In wt zygotes, the FSM accumulated as hemispherical structures beside the ends of spindles (the SPBs) as the two spindle microtubules assembled from prophase II to metaphase II (Fig. 3D,G; supplementary material Movie 1). At anaphase II, during which time spindles elongate, the FSM expanded longitudinally and finally enclosed four spherical prespores. The hemispherical accumulation of the FSM around SPBs at metaphase II could not be detected or was very weak in *npg1Δ* zygotes (Fig. 3E–G; supplementary material Movie 2). The FSM gradually accumulated from the end of meiosis II (indicated by the breakdown of spindles). FSM signals were blurred spots and developed into amorphous structures (Fig. 3E), and sometimes did not emerge through meiosis II in the *npg1Δ* mutant (Fig. 3F). Four FSM spheres were formed in all wt zygotes examined within 30 min after spindle breakdown, whereas no *npg1Δ* zygote contained four spherical structures even at 30–60 min post meiosis (Fig. 3H). Approximately 50% of postmeiotic *npg1Δ* zygotes contained one to three FSM spheres and the remainder contained no FSM spheres.

The circumferential leading edge of the FSM has been shown to play an important role in guiding the development of the membrane to efficiently encapsulate dividing nuclei. Thus, we simultaneously observed the FSM and its leading edges in the *npg1Δ* mutant. Meu14–GFP constantly labeled the edge, as reported previously (Okuzaki et al., 2003). In wt cells, Meu14–GFP rings were always localized at the circumferences of expanding or closing FSM sacs (Fig. 3I). In contrast, small Meu14–GFP rings, which were not common, often did not associate with mCherry–Psy1 signals in *npg1Δ* cells. Furthermore, Meu14–GFP was frequently attached to closed FSM spheres or FSM debris in the mutant. We further examined the assembly of the leading edge rings using time-lapse imaging. In wt zygotes, Meu14–GFP formed two rings from the ends of the metaphase-II spindle (i.e. SPBs) (Fig. 4A; supplementary material Movie 3). These rings stayed inside the poles of the spindle during metaphase II and then began to constrict at anaphase II, during which time the spindle further elongated, leading to the enclosure of nuclei by the FSM. In *npg1Δ* zygotes, Meu14–GFP signals appeared as several spots (Fig. 4B; supplementary material Movie 4) or smaller rings (Fig. 4C; supplementary material Movie 5) around the SPBs at metaphase II. These spots stayed around the spindle without forming rings even after anaphase II. The smaller rings were not orthogonal to the spindle and were hardly pierced by the spindle (Fig. 4D). These rings expanded to some extent during metaphase II and then constricted. All wt zygotes imaged formed four Meu14–GFP rings with a normal diameter. In contrast, no *npg1Δ* zygote

Journal of Cell Science (2014) 127, 4429–4442 doi:10.1242/jcs.151738

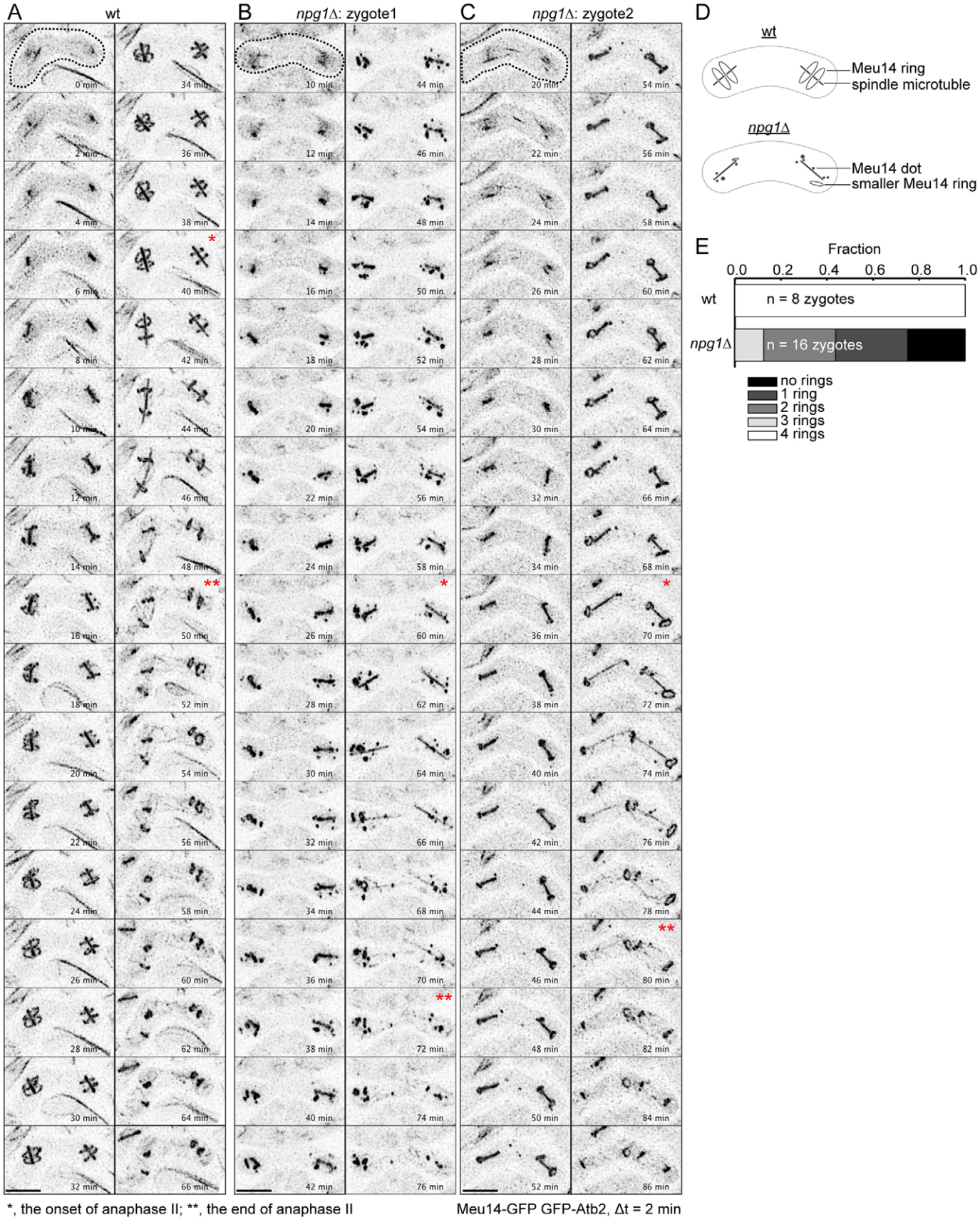

Fig. 4. See next page for legend.

Journal of Cell Science (2014) 127, 4429–4442 doi:10.1242/jcs.151738

Fig. 4. Insufficient development of the leading edges of the FSM in *npg1Δ* cells. (A–C) Time-lapse analysis of the formation of Meu14 rings at the leading edge of the FSM sac. Homothallic wt (A) and *npg1Δ* (B,C) cells expressing both Meu14–GFP and GFP–Atb2 were induced to enter meiosis at 25˚C for 12–14 h, and then imaged. The *z*-stacked images were deconvolved for each time point. Single asterisks indicate the onset of anaphase II, during which spindles began to further elongate. Double asterisks indicate the end of meiosis II, during which time spindles broke down. (D) Schematic representation showing the localization of Meu14 and spindle microtubules in wt and *npg1Δ* cells at anaphase II. (E) Quantification of Meu14 rings in wt and *npg1*Δ asci. The number of Meu14–GFP rings with normal diameters formed in the ascus during time-lapse imaging as shown in A–C was counted. Data were pooled from two independent experiments. Scale bars: 5 μm.

formed four normal Meu14 rings; 80% eventually formed one to three rings with a normal diameter and the remainder formed no rings (Fig. 4E). Taken together, these results indicated that Npg1 is involved in the proper development of leading edge rings and coordinates the association between the FSM and these rings.

Localization of sporulation-related proteins in the absence of Npg1

Several sporulation-specific proteins, including Spo2, Spo7, Spo13 and Spo15, have been shown to localize to meiotic SPBs and to regulate the assembly of the FSM (Nakase et al., 2008; Nakamura-Kubo et al., 2011). We examined the localization of these meiotic SPB components in *npg1Δ* cells (supplementary material Fig. S1A–E). In wt zygotes, Spo15–GFP localized to SPBs during meiosis, and the dot-like signal of Spo15 often appeared as a crescent at metaphase II, whereas it emerged only as dots in the *npg1Δ* mutant. Spo13–GFP localized to meiotic SPBs and occasionally appeared as a crescent in both wt and *npg1Δ* zygotes. Spo7 and Spo2 also localized to meiotic SPBs in both wt and *npg1Δ* zygotes. We also examined the localization of Sad1, a fundamental component of SPBs (Hagan and Yanagida, 1995). Similar to Spo15, Sad1–GFP often appeared as a crescent at metaphase II in wt zygotes, but was hardly present in *npg1Δ* cells (supplementary material Fig. S1F,G). These results indicate that Npg1 is not essential for the localization of Spo2, Spo7, Spo13, Spo15, or Sad1 to the SPBs. The crescent-shaped signal of the SPB components might be derived from the outer plaques formed during meiosis II. Thus, Npg1 might be involved in the organization of these plaques.

Npg1 localized in the vicinity of meiotic spindle pole bodies

To gain mechanistic insights into the function of Npg1, we examined its localization during meiosis. Cells expressing Npg1–GFP or Npg1–3mYFP formed spores as efficiently as cells expressing untagged Npg1, meaning that these tagged proteins were fully functional. We first simultaneously observed the localization of Npg1–3mYFP and Cut11–3mRFP (Fig. 5A). At the horsetail stage and during meiosis I, Npg1 showed no specific localization, which was consistent with its expression profile (Fig. 1). After meiosis I, during which time the zygotes have two nuclei, Npg1 emerged as small dot(s) that almost made contact with the nuclear envelope. As meiosis II progressed, Npg1 formed two dots and localized around the two poles of the dividing nucleus at early anaphase II. Npg1 signals gradually diffused again after meiosis II (Fig. 5A).

The dot localization of Npg1 prompted us to suspect that it was localized to SPBs. Therefore, we simultaneously observed Npg1–3mYFP and Sid4–4mCherry, which labels SPBs. Unexpectedly, Npg1 did not localize to the SPBs in binuclear cells after meiosis I, even though the Npg1 dots were in the vicinity of SPBs (supplementary material Fig. S2A,B). Using higher-resolution imaging, we confirmed that Npg1–3mYFP was present as dot(s) in the nucleus and on the nuclear envelope during the early stages of meiosis II (Fig. 5B).

The Npg1–3mYFP signal was weak; therefore, it was hard to determine its localization after metaphase II. To circumvent this difficulty, we used *npg1Δ* strains expressing Npg1–GFP from the *leu1-32* locus under the control of the *npg1* promoter. The heterotropic expression of Npg1–GFP restored the insufficient sporulation observed in *npg1Δ* cells (see Fig. 7) and somehow provided a brighter signal, which might be attributed to a higher expression level due to the chromosomal position effect at the *leu1* locus (see, for example, Keeney and Boeke, 1994). Similar to Npg1–3mYFP, Npg1–GFP also formed dots distinct from the SPBs in zygotes at post meiosis I, and clearly localized to SPBs during metaphase II to anaphase II (Fig. 5C). Npg1–GFP signals diffused in the prespores and then disappeared.

We further examined changes in the localization of Npg1 using time-lapse imaging. We found that a portion of Npg1–GFP gradually accumulated in the SPBs before and after their separation (Fig. 5D). Before metaphase II, during which time the distance between two SPBs was nearly constant, the translocation of Npg1 to SPBs was completed, and the Npg1–GFP signal was slightly diffused. Kymograph analysis revealed that the dot(s) of Npg1–GFP and SPBs moved independently of each other before metaphase II (Fig. 5E). These results indicate that the recruitment of Npg1 molecules from the subnuclear dots to the SPBs occurs around the onset of metaphase II.

We also observed the localization of Npg1–GFP during expansion of the FSM. Simultaneous observations of Npg1–GFP and mCherry–Psy1 revealed that Npg1 accumulated in the incipient FSM and hemispherical FSMs at metaphase II (Fig. 5F). Npg1–GFP localized very weakly to the almost closed FSM and delocalized from the mostly spherical FSM. Therefore, Npg1–GFP can also localize to the developing FSM, at least when expressed abundantly.

The intranuclear GFP- or 3mYFP-tagged Npg1 often appeared as two or three dots, not only as a single dot. Time-lapse imaging revealed that the number of Npg1–GFP dots fluctuated at between one and three within several minutes (Fig. 5D). These results demonstrate that the Npg1–GFP signal was composed of smaller and disintegrable subunits.

We also investigated whether Npg1 colocalized with the actin cytoskeleton, because it is a potential actin-binding protein. The actin cytoskeleton was successfully visualized using the actin marker Lifeact, as previously reported (Takaine et al., 2014) (supplementary material Fig. S2C–F). After meiosis I, the actin cytoskeleton was mostly composed of cortical actin patches, which did not associate with the intranuclear dots of Npg1. During meiosis II, actin assembled into meiotic actin rings at the leading edges of the FSM (Petersen et al., 1998; Itadani et al., 2006; Yan and Balasubramanian, 2012), whereas Npg1 localized to the SPBs or on the FSM. Importantly, the nascent actin rings, which comprise a few foci of the actin signal, emerged from the immediate vicinity of the Npg1-localized SPB, but did not appear to be localized on the SPBs (supplementary material Fig. S2D,E). As prespores matured, Npg1 disappeared from the spore membrane, whereas actin was seen as cortical patches in the spores. These results indicate that Npg1 scarcely interacted with actin filaments or did not directly modulate the actin structures.

Npg1–GFP exhibited dot localization and localized to the meiotic SPBs in *spo2*, *spo7*, *spo13*, and *spo15* mutants (supplementary

Journal of Cell Science (2014) 127, 4429–4442 doi:10.1242/jcs.151738

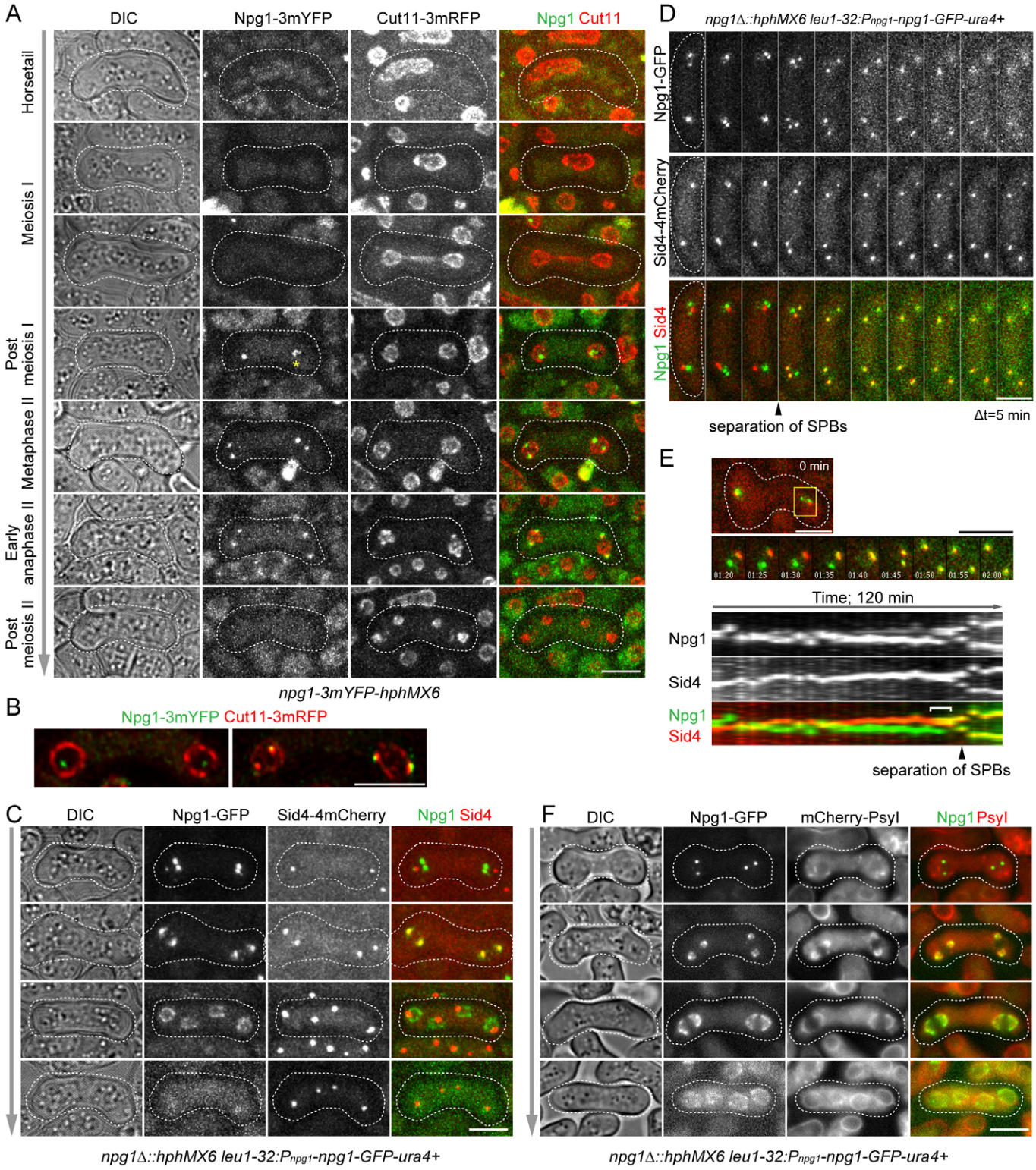

Fig. 5. See next page for legend.

material Fig. S3A). Thus, the localization of Npg1 was independent of these meiotic SPB components. In *spo3Δ* cells, during which FSM assembly halted halfway, Npg1–GFP localized as dots and displayed cup-like structures, but did not diffuse away, suggesting that the delocalization of Npg1 from SPBs required assembly of the FSM (supplementary material Fig. S3B).

Ectopically expressed Npg1 could localize in the nucleus and interfere with sporulation

To further understand the functional properties of the Npg1 protein, we overexpressed Npg1 cDNA in vegetative haploid cells from a plasmid. The overexpression of Npg1 led to formation of a large number of elongated cells (Fig. 6A), whereas cells bearing

Journal of Cell Science (2014) 127, 4429–4442 doi:10.1242/jcs.151738

Fig. 5. Npg1 localized in the nucleus and meiotic spindle pole bodies. (A) Localization of Npg1 during meiosis and sporulation. Homothallic cells expressing Cut11–3mRFP and Npg1–3mYFP were cultured on ME plates at 25°C to induce conjugation and meiosis for 12–14 h before imaging. An asterisk indicates multiple Npg1–3mYFP dots. (B) Npg1 localized to the intranuclear region and nuclear envelope. Zygotes at the early stages of meiosis II were imaged as in A, but with half the resolution. Images were deconvolved, and the maximum projections of the medial three (left) or nine (right) *z*-sections spaced at 0.3 μm intervals are shown. (C) Npg1 transiently localized to meiotic SPBs. Cells expressing Sid4–4mCherry and Npg1–GFP were induced to undergo meiosis. Cell images are arranged according to the meiotic stages. (D) Translocation of Npg1. A zygote was imaged after meiosis I. The arrowhead indicates the separation of SPBs (transition from prophase II to metaphase II). (E) Kymographs of Npg1–GFP. Top, A zygote was imaged for 2 h during meiosis II. (middle) Enlarged time-lapse images of the boxed region shows Npg1–GFP gradually accumulated to duplicated SPBs before they separated. Bottom, kymographs of time-lapse images of the boxed region (each frame was horizontally compressed). A parenthesis indicates the gradual targeting of Npg1 to SPBs. (F) Npg1 could localize to developing FSM. Zygotes expressing mCherry–Psy1 and Npg1–GFP were imaged during meiosis II in a single focal plane. Cell images are arranged according to the development of FSM. Scale bars: 5 μm.

the same plasmid had normal cell lengths when expression from the plasmid was repressed. Although the elongated cells often had one or two globular nuclei and sometimes had a collapsed nucleus (asterisk in Fig. 6A), they persistently proliferated. The intranuclear deposition of Npg1 might have affected the structure of the nucleus and retarded mitosis or cytokinesis, but did not completely suppress them, without inhibiting cell growth.

We next observed the localization of Npg1 in vegetative cells moderately overexpressing mYFP–Npg1. Ectopically expressed Npg1 accumulated selectively in the nucleus and appeared as several foci (Fig. 6B). These foci localized both on the nuclear envelope and in the intranuclear region, but did not associate with SPBs. These results indicated that the Npg1 protein could intrinsically accumulate in the nucleus, but not in the SPBs, and localized as dots.

We also examined whether the overexpression of Npg1 affected spore formation. The overexpressed Npg1 in diploid cells was also concentrated in the nucleus and diffusely over the cytoplasm (Fig. 6C). The efficiency of sporulation in Npg1-overexpressing diploid cells was markedly impaired (Fig. 6D). Therefore, the constitutive expression of Npg1 from premeiotic stages disturbs the progression of sporulation.

The N-terminal region of Npg1 is required for its localization, whereas the C-terminal region is essential for proper sporulation

As Npg1 contained no conserved domains, except for the CHD, the functional dissection of its entire length was desirable. Therefore, we constructed several deletion forms of Npg1–GFP (Fig. 7A). These mutant *npg1-GFP* genes were introduced into the original locus or the *leu1-32* locus in *npg1Δ* cells and expressed under the control of its own promoter. Although the deletion of C-terminal regions spanning amino acids 100–400 reduced the efficiency of sporulation to the equivalent to that of the *npg1Δ* strain, these truncated Npg1–GFP proteins showed normal localization patterns (Fig. 7B–D). Therefore, the C-terminal region is implicated Npg1 function, but not its localization. Furthermore, we mapped the regions necessary for the proper localization of Npg1 to the first 66 amino acids and an ~370-amino-acid region corresponding to amino acids 169–535 (Fig. 7A). The deletion of the CHD moiety did not affect the localization of Npg1, but partially reduced the efficiency of sporulation, which suggested that the CHD is involved in the role of Npg1 in spore formation.

Genetic interactions between *npg1*-null and sporulation-related genes

To elucidate the relationships between Npg1 and known sporulation-related proteins, we examined several sporulation mutants to determine whether they displayed a synthetic phenotype in combination with *npg1Δ*. We found that the severity of the spore formation defect of *npg1Δ* was enhanced in *spo3-GFP npg1Δ* cells as they were substantially unable to form spores, whereas sporulation was only slightly compromised in *spo3-GFP npg1*$^{+}$ (supplementary material Fig. S4A,B; Nakamura et al., 2001). These results suggested a genetic interaction between *npg1* and *spo3*. We examined the localization of Spo3–GFP during the formation of prespores. Spo3–GFP accumulated around nuclear envelopes in wt zygotes after metaphase II and formed four spheres that encapsulated nuclei, similar to Psy1 (supplementary material Fig. S4C). In contrast, in *npg1Δ* zygotes, Spo3–GFP only slightly accumulated at metaphase II and eventually formed some aggregates that were dissociated from nuclei. We also demonstrated that *npg1Δ meu14Δ* cells were unable to form spores (supplementary material Fig. S4D,E). Given that *meu14Δ* generated an additive effect with *npg1Δ* in sporulation, they might function independently or only partially collaborate.

DISCUSSION

Possible signal transduction from the nucleoplasm to SPBs upon sporulation

In the present study, we showed that the fission yeast protein Npg1 is involved in sporulation and exhibited a characteristic translocalization (Fig. 8A). Npg1 was exclusively produced after meiosis I, possibly under the control of Mei4 through the two FLEX elements located in the 5′ untranslated region (UTR), and localized in the nuclei as multiple dots. Between prophase II and metaphase II, during which duplicated SPBs separated in the nucleus, Npg1 gradually translocated to the SPBs. As the FSM expanded, Npg1 also spread over the membrane and dispersed into prespores. We speculate that the Npg1–GFP or Npg1–3mYFP signals expressed by the endogenous locus might have been undetectable on the FSM simply because they were below the detection limit.

Even when it was ectopically expressed in vegetative cells, Npg1 also accumulated in the nucleus, not in the SPBs, which indicated that the intranuclear localization of Npg1 was intrinsic to the protein. In contrast, the SPB localization of Npg1 might require the activities of associated proteins that are specifically produced at meiosis. We revealed that two N-terminal regions were indispensable for the localization of Npg1. However, the molecular basis for this localization remains unclear because Npg1 has no conserved localization domain or signal sequence. Given that Npg1 is a basic protein, and the region is also rich in basic amino acids, some of these residues might be involved in the nuclear transportation of Npg1. Npg1 sometimes appeared as a composite of one to three smaller dots, which suggests that there is a hierarchical aggregation of these molecules. Alternatively, Npg1 might be highly concentrated at a constant number of discrete subnuclear structures such as chromosomes.

At metaphase II, timely post-translational modifications (e.g. phosphorylation) in the Npg1 protein or some Npg1-binding proteins might lead to the accumulation of intranuclear Npg1 in

Journal of Cell Science (2014) 127, 4429–4442 doi:10.1242/jcs.151738

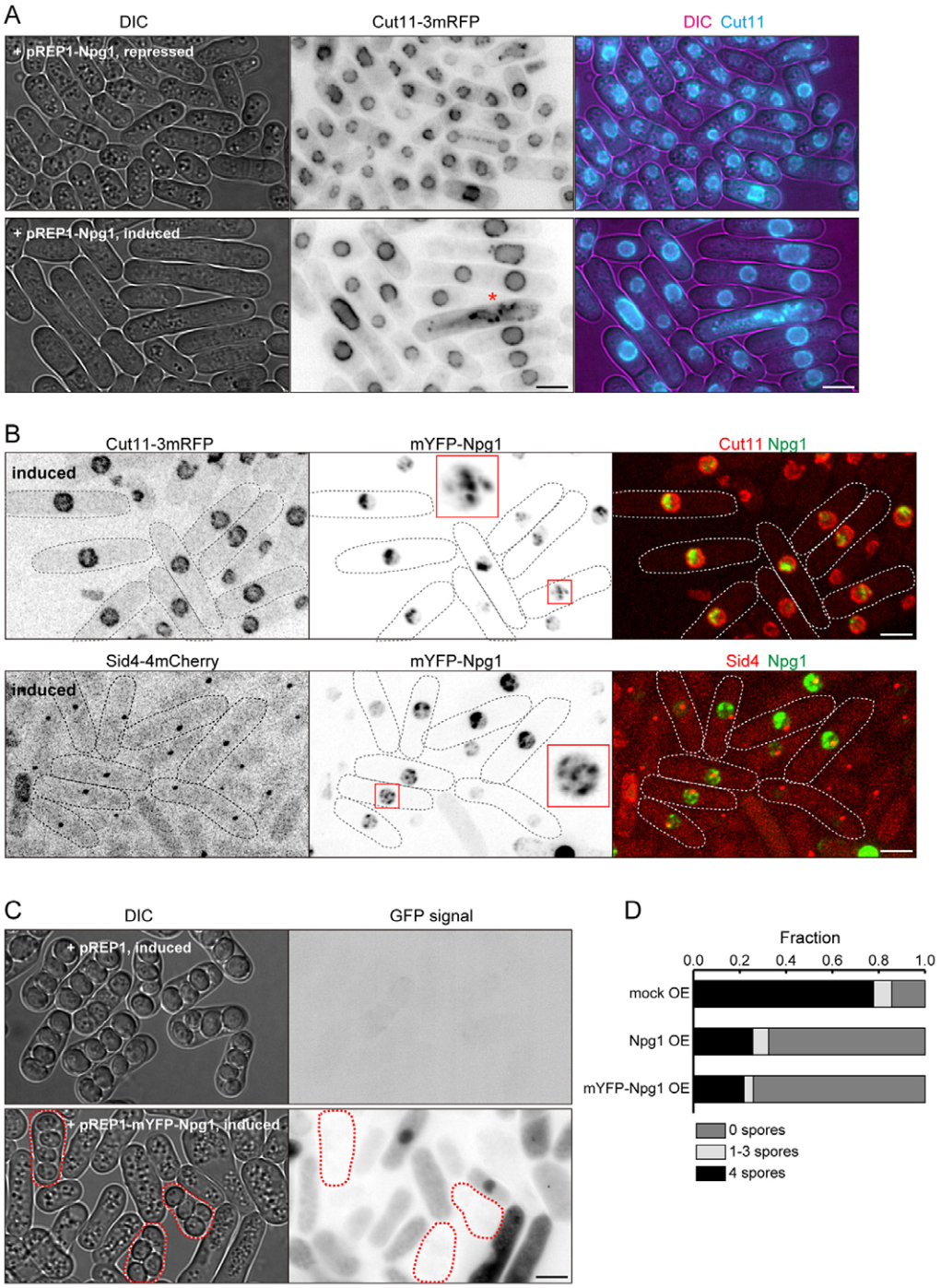

Fig. 6. Ectopically expressed Npg1 could localize to the nucleus and interfere with sporulation. (A) The overexpression of Npg1 in vegetatively growing cells. Cells expressing Cut11–3mRFP were transformed with pREP1-Npg1, grown to the mid-log phase in the presence (repressed) or absence (induced) of 5 μM thiamine for 29 h at 30℃, and then imaged in a single focal plane. The asterisk indicates a cell with an abnormally dispersed nuclear envelope. (B) Ectopically expressed Npg1 selectively localized in the nucleus. Cells expressing Cut11–3mRFP or Sid4–4mCherry were transformed with pREP1-mYFP-Npg1 and grown in the absence of thiamine for 18 h at 25℃ before imaging. Insets show 2.7-times magnified images of the boxed regions. (C) The overexpression of Npg1 inhibited sporulation. Diploid cells (MTY120) were transformed with pREP1 or pREP1-mYFP-Npg1 and grown in the absence of thiamine for 24 h at 25℃. These cells were starved of nitrogen for 16–18 h at 25℃ to induce meiosis and sporulation, and then imaged in a single focal plane. The expression levels of mYFP–Npg1 were lower in sporulating cells (outlined) than in non-sporulating cells. (D) Quantification of the number of spores per ascus of Npg1-overexpressing cells. More than 1100 asci from two independent experiments were scored for each construct. Scale bars: 5 μm.

SPBs. The delocalization of Npg1 from SPBs depended on the assembly of the FSM itself. Thus, after anaphase II, Npg1 might associate weakly with the FSM and diffuse over the membrane accompanying its expansion. This is supported by the partial dispersion of Npg1 from SPBs after anaphase II in *spo3Δ* cells, during which FSM assembly was initiated, but not completed.

Journal of Cell Science (2014) 127, 4429–4442 doi:10.1242/jcs.151738

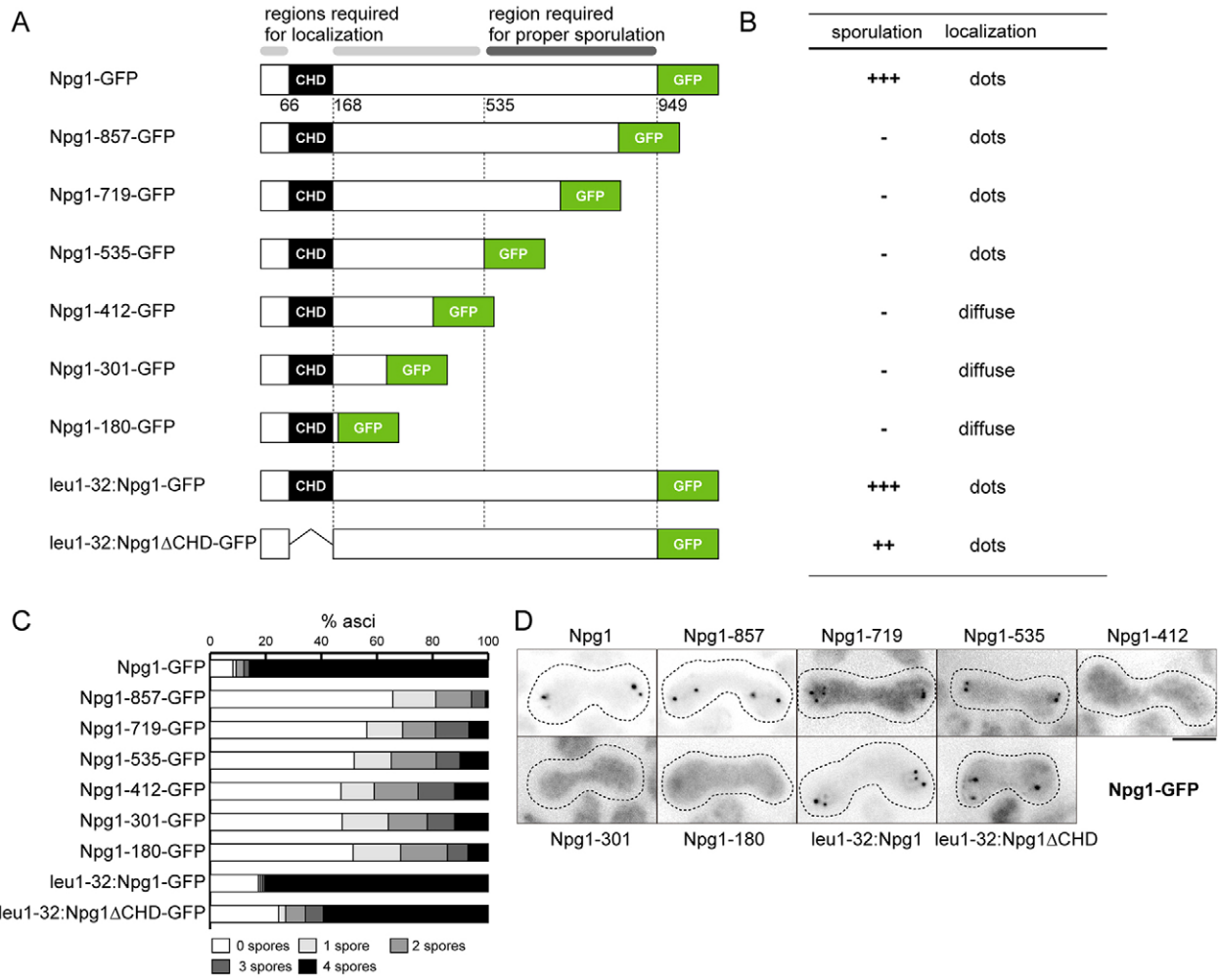

Fig. 7. Distinct roles of the N- and C-terminal regions of Npg1. (A) Diagram of the *npg1* deletion mutants. 'leu1-32' means that the construct was expressed from the *leu1-32* locus under the *npg1Δ* background. (B) Summary of the function and localization of the mutant Npg1 proteins. The functionality of the Npg1 constructs was assessed by their ability to produce four normal spores (shown in C). (C) Quantification of the number of spores per ascus of the *npg1* mutants. Homothallic cells expressing mutant Npg1–GFP were incubated on an ME plate at 25℃ for 2 days. More than 500 asci from two independent preparations were scored for each strain. (D) Cells expressing mutant Npg1–GFP were induced to undergo meiosis and imaged in a single focal plane. Scale bar: 5 μm.

Owing to the limited resolution of the optical microscope, we were unable to determine whether Npg1 attached to the SPBs implanted through the nuclear envelope from the nucleoplasmic or cytoplasmic side after nuclear export. By contrast, the colocalization of Npg1 with the FSM undoubtedly indicates that Npg1 was exported outside the nucleus by that time. The mechanism underlying the nuclear export of Npg1 remains unknown. Previous studies have reported that the permeability of the nuclear envelope increases transiently during anaphase II and some nuclear proteins actually disperse from the nucleus (Arai et al., 2010; Asakawa et al., 2010). Therefore, Npg1 might also diffuse outside the nucleus at anaphase II or might leak to the cytoplasm through the partially permeabilized nuclear envelope during prophase II or metaphase II.

The localization of Npg1 was independent of the meiotic SPB components essential for FSM assembly, such as Spo2, Spo7, Spo13 and Spo15. Reciprocally, these proteins localized normally to the SPBs in *npg1Δ* cells. Spo2, Spo13, Spo15 and Spo7 have been shown to localize at the cytoplasmic side of SPBs throughout meiosis, with the former three forming a tight, hierarchical complex using Spo15 as an initial core (Nakase et al., 2008). Thus, Npg1 might accumulate and localize to meiotic SPBs using a system that is different from the Spo15- or Spo7-dependent ones. Alternatively, Npg1 might simply localize at the opposite, nucleoplasmic, side of SPBs.

The spatial separation of Npg1 from other proteins involved in sporulation until metaphase II might be related to its function. As discussed below, Npg1 might contribute to the initial assembly of the FSM from the vicinity of SPBs at early metaphase II and the concurrent formation of its leading edge rings. Therefore, the localization of Npg1 to SPBs at that time would be consistent with such a function. Subnuclear sequestration might be necessary for Npg1 to precisely sense the meiotic phase and avoid the untimely and, hence, deleterious unleashing of its activity, which was observed in Npg1-overexpressing asci. Collectively, the translocalization of Npg1 implies that some temporal signal from the nucleus could be transduced to meiotic SPBs for the punctual assembly of the FSM.

Some sporulation-related proteins also translocate from the nucleus to the cytoplasm. Spo20, a phosphatidylinositol- and

Journal of Cell Science (2014) 127, 4429–4442 doi:10.1242/jcs.151738

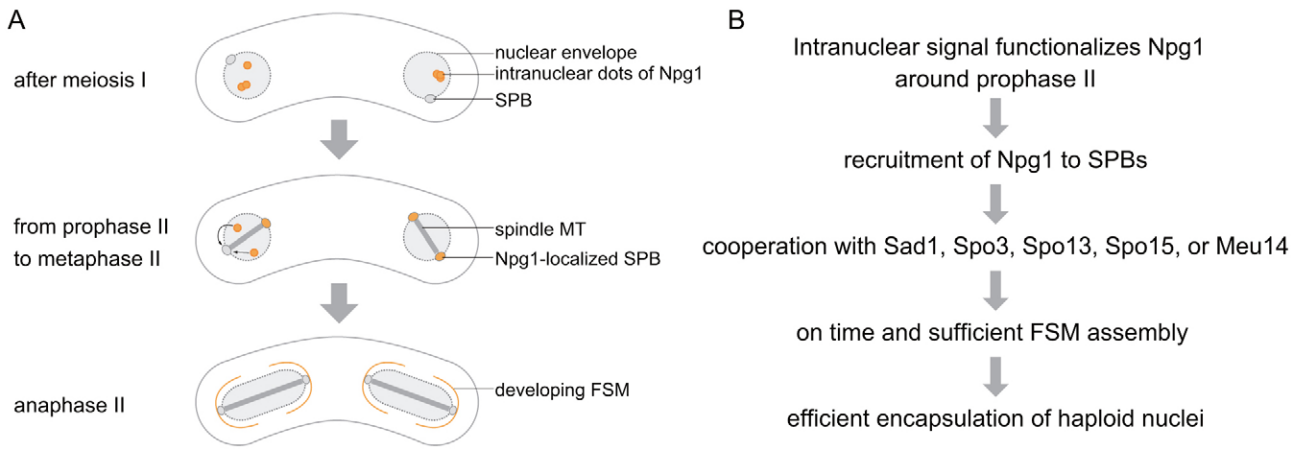

Fig. 8. Models for the localization and function of Npg1. (A) Schematic summary of the localization of Npg1 during meiosis. After meiosis I, Npg1 (orange) emerges as intranuclear dots distinct from the SPBs, and gradually transferred to segregated SPBs after prophase II. Npg1 spread over the membrane upon the initiation of FSM assembly. (B) A possible role of Npg1 in the formation of the FSM. At around prophase II, intranuclear Npg1 is stimulated by an internal signal, and translocated to the SPBs. The SPB-localized Npg1 cooperates with Sad1, Spo3, Spo13, Spo15, and Meu14 to induce the sufficient accumulation of the FSM and correct organization of its leading edge rings.

phosphatidylcholine-transfer protein essential for viability (Sec14 in *S. cerevisiae*), has been implicated in the formation of the FSM and translocates from the nucleus to the FSM (Nakase et al., 2001). The meiosis-specific Sid2-related kinase Slk1/Mug27 has been shown to regulate FSM assembly, and it localizes to the SPB after meiosis I and then moves over the FSM during meiosis II (Ohtaka et al., 2008; Pérez-Hidalgo et al., 2008; Yan et al., 2008). The meiosis-specific transcription factor Cuf2 regulates the expression of several meiotic genes and is exported from the nucleus to the cytoplasm during sporulation (Ioannoni et al., 2012). Npg1 might translocate and partially harness the mechanisms used by these proteins or might interact with them.

Function of Npg1 in FSM assembly

The assembly of the FSM was observed in *npg1Δ* zygotes, but was severely impaired. The accumulation of the FSM at metaphase II was insufficient to form cup-like structures. Inevitably, FSM assembly was markedly delayed and ectopic in the mutant, often causing the unsuccessful envelopment of nuclei. The inefficient formation of prespores undoubtedly decreased the mean number of spores produced. The reduced viability of spores derived from *npg1Δ* asci might be due to the low abundance of FSM materials, which would diminish the volume of sporeplasm and, hence, affect spore maturation. Given the localization of Npg1 at the SPBs in metaphase II, Npg1 might contribute to the concentration and shaping of FSM precursors, and also to the precise launch of their expansion at the onset of anaphase II. However, we could not exclude the possibility of the intranuclear functioning of Npg1.

The formation and spatial arrangement of the leading edge rings of the FSM were also compromised in *npg1Δ* cells. These rings were previously shown to be indispensable for the proper organization of the FSM, but not necessarily a prerequisite for membrane assembly (Okuzaki et al., 2003). Thus, Npg1 might be independently involved in the accumulation of the FSM as well as in the organization of its leading edges. The reduced accumulation of the FSM and improper formation of its circumference might synergistically cause insufficient prespore formation. Based on the genetic relationship between Npg1 and Meu14, they might function in parallel, but not in the same pathway, to appropriately organize the leading edge rings. Meu14 has been shown to localize to SPBs at prophase II and form rings at metaphase II (Nakamura-Kubo et al., 2011). Npg1 might interact with other, as-yet-unidentified component(s) of the leading edge at SPBs. Given that the ring initially emerged by expanding from the spindle pole (not *de novo*) in wild-type cells (Fig. 4A), SPB-localized Npg1 might modulate the prototypic shape of the ring.

npg1Δ exhibited a negative genetic interaction with spo3–GFP and the aberrant localization of Spo3. The function of Spo3–GFP in sporulation might be slightly compromised as previously reported (Pérez-Hidalgo et al., 2008; Yan et al., 2008; Li et al., 2010), and might also be further deteriorated by a loss in the function of Npg1. This again supports the involvement of Npg1 in the initial assembly of the FSM because Spo3 has been implicated in the later development of the FSM (Nakamura et al., 2001) and, hence, the entire process of FSM formation might be impaired in the double mutant.

Spo15–GFP and Sad1–GFP, which localized on the SPBs, hardly ever showed a crescent form in *npg1Δ* cells, whereas this was observed in *spo13Δ* cells (Nakase et al., 2008). Previous studies using electron microscopy have suggested that the crescent signal of Spo15 might represent the meiotic outer plaque formed at the cytoplasmic side of the SPBs. This plaque is indispensable for FSM assembly, with Spo15 being required for plaque formation (Ikemoto et al., 2000; Nakase et al., 2008). Given the partially compromised sporulation in *npg1Δ* cells, the plaque might be incompletely formed in the mutant, as was also observed in the *spo13Δ* mutant (Nakase et al., 2008), thereby leading to a reduction in the accumulation of FSM. Npg1 might independently modify the localization of Spo15 and Sad1 at meiotic SPBs or in collaboration with Spo13. A possible role of Npg1 is depicted in Fig. 8B.

The function of the CHD of Npg1 remains unclear because Npg1 showed no colocalization with the actin cytoskeleton and the deletion of CHD only slightly altered the function of the protein. As the C-terminal region, rather than the N-terminal region containing the CHD, might be directly involved in the function of Npg1 for sporulation (Fig. 7), Npg1 might interact with Spo3, Spo13, Spo15 or the leading edge through this region.

However, a protein database search did not result in the identification of the counterparts of Npg1 in other species apart from some fission yeasts. Therefore, the functional homologs of Npg1 in other eukaryotes might play a role in the accurate compartmentalization of haploid nuclei and its tight coordination with meiotic nuclear division during sporulation or intracellular gametogenesis.

MATERIALS AND METHODS

Yeast strains and culture conditions

The fission yeast strains and oligonucleotide primers used in this study are listed in supplementary material Tables S1 and S2, respectively. These strains were constructed by a PCR-sewing method (Matsuyama et al., 2000) using pFA6-based plasmids (Bähler et al., 1998) and its derivatives as PCR templates, and by genetic crosses. Cells were grown in complete yeast extract medium (YES) or in minimal medium (EMM) with auxotrophic supplements. Cells were incubated on malt extract (ME) plates or cultured in EMM lacking a nitrogen source (EMM-N) at 25℃ for mating and sporulation. To induce asynchronous mating and meiosis, homothallic (h^{90}) cells were grown to the mid-log phase in YES liquid medium at 25℃, washed with water, and were spotted onto ME plates and incubated for 12–14 h at 25℃. Zygotes in the culture, which were mostly at meiosis, were subjected to microscopy. Synchronous meiosis in a *pat1-114* temperature-sensitive mutant was induced as previously reported (Kitajima et al., 2003) . Briefly, *pat1-114* cells were exponentially grown in YES medium. The cells were resuspended in EMM-N plus supplements at an optical density at 595 nm (OD_{595})=0.3 and then cultured for 15 h at 25℃. The culture was shifted to 34℃ to inactivate the mutant Pat1 kinase and induce enforced meiosis. Exogenous constructs were expressed under the thiamine-repressible *nmt1* promoter on a multi-copy plasmid pREP1.

To generate an *npg1Δ* strain, the entire open reading frame (ORF) of *npg1*$^{+}$ was replaced in a haploid strain with the *kanMX6* cassette using PCR-based gene targeting to obtain the strain *npg1Δ::kanMX6*. The *npg1Δ::hphMX6* strain was constructed from the *npg1Δ::kanMX6* strain using a one-step marker switch method (Sato et al., 2005).

For Npg1–GFP or Npg1−3mYFP tagging, a DNA fragment consisting of 400 bp of the end of the Npg1 ORF, GFP, or 3mYFP-3HA tag flanked by the drug-resistant cassette, and 400 bp of the Npg1 3′ UTR was amplified by a high-fidelity DNA polymerase, PrimeSTAR Max (TaKaRa, Japan) using the primers npg1F3 and npg1R3 or npg1F3 and npg1R8 from pFA6a-GFP-kanMX6 or pFA6a-3mYFP-3HA-hphMX6, respectively. Four or five glycine linkers were introduced between the fluorescent proteins and the end of the Npg1 ORF (without the stop codon). To generate truncation mutant strains of Npg1 (MTY765-769 and MTY751), GFP tags flanked by the *hphMX6* cassette were amplified using appropriate primers and inserted after amino acids 857, 719, 535, 412, 301 and 180 of endogenous Npg1, respectively.

For the expression of Npg1–GFP or Npg1ΔCHD–GFP from the *leu1-32* locus, MTP798 or 799 was linearized by *Xho*I cutting and integrated into the *leu1-32* locus of *npg1Δ::hphMX6* strain. Stable transformants were isolated by uracil prototrophy to yield MTY758 and MTY762, respectively. All gene deletions or integrations were confirmed by diagnostic PCR. In all the strains expressing Npg1–GFP or its derivatives (from the endogenous locus or from the *leu1-32* locus) used in this study, the original 3′ UTR of the *npg1* gene was not conserved, but was replaced by the terminator sequence of the *ADH1* gene from *S. cerevisiae* (abbreviated as T_{ADH1}) derived from pFA6a plasmids. However, the modification of the 3′ UTR did not appear to affect the meiosis-specific upregulation of the *npg1*$^{+}$ gene and the suppression in vegetative cells, as evidenced by the data shown in Fig. 1B–D and supplementary material Fig. S2C.

Plasmid construction

The plasmids used in this study are listed in supplementary material Table S3. The full-length cDNA of *npg1*$^{+}$ was amplified by PCR using the DNA polymerase KOD FX (TOYOBO, Japan) and primers npg1-cloS1 and npg1-cloAS2 from a cDNA library. The product was cut by *Sal*I and *BamH*I, and subcloned into the expression vector pREP1 to yield pKI203. An *Nde*I–*Xho*I fragment of mYFP was ligated into the *Nde*I/*Sal*I sites of pKI203 to yield MTP813.

We amplified the Npg1–GFP ORF flanked by the promoter of *npg1* (corresponding to the 5′ UTR from −250 to −1, relative to the transcription start site, abbreviated as P_{npg1}) and the terminator T_{ADH1} from the genomic DNA of Npg1–GFP cells (MTY741) in two segments: the 5′ segment with primers npg1F7 and npg1R11 and the 3′ segment with primers npg1F8 and Tadh1R1. These segments were inserted by trimeric ligation into the *leu1-32* integration vector MTP75 to create MTP798. The resultant plasmid contained a gene expression module P_{npg1}-*npg1-GFP*-T_{ADH1}-*ura4*$^{+}$. To create MTP799, residues corresponding to the CHD moiety (amino acids 66–168) were removed from MTP798 using a PrimeSTAR mutagenesis kit (TaKaRa) and the primers npg1F13 and npg1R15, yielding an expression module P_{npg1}-*npg1ΔCHD-GFP*-T_{ADH1}-*ura4*$^{+}$. All plasmids were sequenced to confirm PCR fidelity.

Microscopy

Single time-point and epifluorescence microscopy was performed as previously reported (Takaine et al., 2014) using a fluorescence microscope (BX51; Olympus, Japan) equipped with a Plan-Apo 100×/1.40 NA objective lens (Olympus) using a cooled charge-coupled device camera (ORCAII-ER-1394; Hamamatsu Photonics, Japan) and SimplePCI software (Hamamatsu Photonics). Time-lapse imaging was performed under a confocal microscope (LSM 700; Carl Zeiss, Inc.) equipped with an alpha Plan-Apochromat 100×/1.46 NA objective lens (Carl Zeiss, Inc., Germany) at room temperature (20–25℃). Cells for time-lapse imaging were immobilized on pads made from 25% gelatin in media as described previously (Wu et al., 2008). Stacks of 12–17 confocal *z*-sections spaced by 0.3–0.5 µm were typically collected. The stack of *z*-sections was projected to an *x*-*y* image using a maximum intensity projection unless otherwise noted. To increase the signal to noise ratio, *z*-sections were sometimes smoothened with a Gaussian blur filter using ImageJ software before the projection or were sometimes deconvolved using Huygens Essential software (ver. 4.5; Scientific Volume Imaging, Netherlands). Spindle microtubules were visualized by GFP–Atb2 to monitor meiosis. Nuclei were stained with 1 µg/ml DAPI or 5 µg/ml Hoechst 33342.

Spore viability

Homothallic wt and *npg1Δ* strains were incubated on ME plates for 3–4 days at 25℃ to allow cells to fully mate and sporulate. Normal-looking spores liberated from asci were randomly chosen and separated on a YE plate using a micromanipulator (Singer Instruments, UK). These plates were incubated for 4 days at 30℃, and the colonies that formed were examined.

Immunoblotting

Total cell lysates were prepared as described previously (Masai et al., 1995). Proteins were resolved by SDS-PAGE and transferred onto a polyvinylidene difluoride membrane (Immobilon-P; Millipore). GFP and α-tubulin were probed using an anti-GFP antibody (Roche, Switzerland) and the anti-tubulin antibody TAT-1 (Woods et al., 1989) as the primary antibodies, respectively. A horseradish-peroxidase-conjugated goat anti-mouse-IgG antibody (Santa Cruz Biotechnology) was used as the secondary antibody, and immunoreactive bands were detected using an enhanced chemiluminescence detection kit (ECL advance, Amersham Biosciences, Sweden).

Acknowledgements

We are grateful to Rikuri Morita (University of Tsukuba) for assisting with the initial stage of this research, and Akira Yamashita (National Institute for Basic Biology), Masamitsu Sato (Waseda University) and the Yeast Genetic Resource Center for providing yeast strains or valuable suggestions.

Competing interests

The authors declare no competing interests.

Author contributions

M.T. and K.N. designed the research with contributions from T.N., K.I. and O.N. M.T. and K.I. conducted the experiments. M.T. wrote the paper with contributions from all other authors.

Funding

This work was supported by a Grant-in-Aid for Scientific Research from the Ministry of Education, Culture, Sports, Science and Technology (MEXT) [grant numbers 19037004 and 20770150 to K.N., 24570219 to T.N.]; and by a Grant-in-Aid for Young Scientists (B) (JSPS KAKENHI) [grant number 24770177 to M.T.]. K.I. is a recipient of the Research Fellowship for Young Scientists from the Japan Society for the Promotion of Science.

Supplementary material

Supplementary material available online at
http://jcs.biologists.org/lookup/suppl/doi:10.1242/jcs.151738/-/DC1

References

Arai, K., Sato, M., Tanaka, K. and Yamamoto, M. (2010). Nuclear compartmentalization is abolished during fission yeast meiosis. *Curr. Biol.* **20**, 1913-1918.

Asakawa, H., Kojidani, T., Mori, C., Osakada, H., Sato, M., Ding, D. Q., Hiraoka, Y. and Haraguchi, T. (2010). Virtual breakdown of the nuclear envelope in fission yeast meiosis. *Curr. Biol.* **20**, 1919-1925.

Bähler, J., Wu, J. Q., Longtine, M. S., Shah, N. G., McKenzie, A., III, Steever, A. B., Wach, A., Philippsen, P. and Pringle, J. R. (1998). Heterologous modules for efficient and versatile PCR-based gene targeting in Schizosaccharomyces pombe. *Yeast* **14**, 943-951.

Eng, K., Naqvi, N. I., Wong, K. C. and Balasubramanian, M. K. (1998). Rng2p, a protein required for cytokinesis in fission yeast, is a component of the actomyosin ring and the spindle pole body. *Curr. Biol.* **8**, 611-621.

Gimona, M., Djinovic-Carugo, K., Kranewitter, W. J. and Winder, S. J. (2002). Functional plasticity of CH domains. *FEBS Lett.* **513**, 98-106.

Goyal, A., Takaine, M., Simanis, V. and Nakano, K. (2011). Dividing the spoils of growth and the cell cycle: The fission yeast as a model for the study of cytokinesis. *Cytoskeleton (Hoboken)* **68**, 69-88.

Hagan, I. and Yanagida, M. (1995). The product of the spindle formation gene sad1+ associates with the fission yeast spindle pole body and is essential for viability. *J. Cell Biol.* **129**, 1033-1047.

Hiraoka, Y. (1998). Meiotic telomeres: a matchmaker for homologous chromosomes. *Genes Cells* **3**, 405-413.

Horie, S., Watanabe, Y., Tanaka, K., Nishiwaki, S., Fujioka, H., Abe, H., Yamamoto, M. and Shimoda, C. (1998). The Schizosaccharomyces pombe mei4+ gene encodes a meiosis-specific transcription factor containing a forkhead DNA-binding domain. *Mol. Cell. Biol.* **18**, 2118-2129.

Ikemoto, S., Nakamura, T., Kubo, M. and Shimoda, C. (2000). S. pombe sporulation-specific coiled-coil protein Spo15p is localized to the spindle pole body and essential for its modification. *J. Cell Sci.* **113**, 545-554.

Ioannoni, R., Beaudoin, J., Lopez-Maury, L., Codlin, S., Bähler, J. and Labbe, S. (2012). Cuf2 is a novel meiosis-specific regulatory factor of meiosis maturation. *PLoS ONE* **7**, e36338.

Itadani, A., Nakamura, T. and Shimoda, C. (2006). Localization of type I myosin and F-actin to the leading edge region of the forespore membrane in Schizosaccharomyces pombe. *Cell Struct. Funct.* **31**, 181-195.

Itadani, A., Nakamura, T., Hirata, A. and Shimoda, C. (2010). Schizosaccharomyces pombe calmodulin, Cam1, plays a crucial role in sporulation by recruiting and stabilizing the spindle pole body components responsible for assembly of the forespore membrane. *Eukaryot. Cell* **9**, 1925-1935.

Keeney, J. B. and Boeke, J. D. (1994). Efficient targeted integration at leu1-32 and ura4-294 in Schizosaccharomyces pombe. *Genetics* **136**, 849-856.

Kitajima, T. S., Miyazaki, Y., Yamamoto, M. and Watanabe, Y. (2003). Rec8 cleavage by separase is required for meiotic nuclear divisions in fission yeast. *EMBO J.* **22**, 5643-5653.

Krapp, A., Collin, P., Cokoja, A., Dischinger, S., Cano, E. and Simanis, V. (2006). The Schizosaccharomyces pombe septation initiation network (SIN) is required for spore formation in meiosis. *J. Cell Sci.* **119**, 2882-2891.

Krapp, A., Del Rosario, E. C. and Simanis, V. (2010). The role of Schizosaccharomyces pombe dma1 in spore formation during meiosis. *J. Cell Sci.* **123**, 3284-3293.

Li, W. Z., Yu, Z. Y., Ma, P. F., Wang, Y. and Jin, Q. W. (2010). A novel role of Dma1 in regulating forespore membrane assembly and sporulation in fission yeast. *Mol. Biol. Cell* **21**, 4349-4360.

Masai, H., Miyake, T. and Arai, K. (1995). hsk1+, a Schizosaccharomyces pombe gene related to Saccharomyces cerevisiae CDC7, is required for chromosomal replication. *EMBO J.* **14**, 3094-3104.

Mata, J., Lyne, R., Burns, G. and Bähler, J. (2002). The transcriptional program of meiosis and sporulation in fission yeast. *Nat. Genet.* **32**, 143-147.

Mata, J., Wilbrey, A. and Bähler, J. (2007). Transcriptional regulatory network for sexual differentiation in fission yeast. *Genome Biol.* **8**, R217.

Matsuyama, A., Yabana, N., Watanabe, Y. and Yamamoto, M. (2000). Schizosaccharomyces pombe Ste7p is required for both promotion and withholding of the entry to meiosis. *Genetics* **155**, 539-549.

Murone, M. and Simanis, V. (1996). The fission yeast dma1 gene is a component of the spindle assembly checkpoint, required to prevent septum formation and premature exit from mitosis if spindle function is compromised. *EMBO J.* **15**, 6605-6616.

Nakamura, T., Nakamura-Kubo, M., Hirata, A. and Shimoda, C. (2001). The Schizosaccharomyces pombe spo3+ gene is required for assembly of the forespore membrane and genetically interacts with psy1(+)-encoding syntaxin-like protein. *Mol. Biol. Cell* **12**, 3955-3972.

Nakamura-Kubo, M., Nakamura, T., Hirata, A. and Shimoda, C. (2003). The fission yeast spo14+ gene encoding a functional homologue of budding yeast Sec12 is required for the development of forespore membranes. *Mol. Biol. Cell* **14**, 1109-1124.

Nakamura-Kubo, M., Hirata, A., Shimoda, C. and Nakamura, T. (2011). The fission yeast pleckstrin homology domain protein Spo7 is essential for initiation of forespore membrane assembly and spore morphogenesis. *Mol. Biol. Cell* **22**, 3442-3455.

Nakase, Y., Nakamura, T., Hirata, A., Routt, S. M., Skinner, H. B., Bankaitis, V. A. and Shimoda, C. (2001). The Schizosaccharomyces pombe spo20(+) gene encoding a homologue of Saccharomyces cerevisiae Sec14 plays an important role in forespore membrane formation. *Mol. Biol. Cell* **12**, 901-917.

Nakase, Y., Nakamura-Kubo, M., Ye, Y., Hirata, A., Shimoda, C. and Nakamura, T. (2008). Meiotic spindle pole bodies acquire the ability to assemble the spore plasma membrane by sequential recruitment of sporulation-specific components in fission yeast. *Mol. Biol. Cell* **19**, 2476-2487.

Neiman, A. M. (2011). Sporulation in the budding yeast Saccharomyces cerevisiae. *Genetics* **189**, 737-765.

Ohtaka, A., Okuzaki, D. and Nojima, H. (2008). Mug27 is a meiosis-specific protein kinase that functions in fission yeast meiosis II and sporulation. *J. Cell Sci.* **121**, 1547-1558.

Okuzaki, D., Satake, W., Hirata, A. and Nojima, H. (2003). Fission yeast meu14+ is required for proper nuclear division and accurate forespore membrane formation during meiosis II. *J. Cell Sci.* **116**, 2721-2735.

Onishi, M., Koga, T., Hirata, A., Nakamura, T., Asakawa, H., Shimoda, C., Bähler, J., Wu, J. Q., Takegawa, K., Tachikawa, H. et al. (2010). Role of septins in the orientation of forespore membrane extension during sporulation in fission yeast. *Mol. Cell. Biol.* **30**, 2057-2074.

Pérez-Hidalgo, L., Rozalén, A. E., Martín-Castellanos, C. and Moreno, S. (2008). Slk1 is a meiosis-specific Sid2-related kinase that coordinates meiotic nuclear division with growth of the forespore membrane. *J. Cell Sci.* **121**, 1383-1392.

Petersen, J., Nielsen, O., Egel, R. and Hagan, I. M. (1998). F-actin distribution and function during sexual differentiation in Schizosaccharomyces pombe. *J. Cell Sci.* **111**, 867-876.

Sato, M., Dhut, S. and Toda, T. (2005). New drug-resistant cassettes for gene disruption and epitope tagging in Schizosaccharomyces pombe. *Yeast* **22**, 583-591.

Shimoda, C. (2004). Forespore membrane assembly in yeast: coordinating SPBs and membrane trafficking. *J. Cell Sci.* **117**, 389-396.

Takaine, M., Numata, O. and Nakano, K. (2014). Fission yeast IQGAP maintains F-actin-independent localization of myosin-II in the contractile ring. *Genes Cells* **19**, 161-176.

Tanaka, K. and Hirata, A. (1982). Ascospore development in the fission yeasts Schizosaccharomyces pombe and S. japonicus. *J. Cell Sci.* **56**, 263-279.

Woods, A., Sherwin, T., Sasse, R., MacRae, T. H., Baines, A. J. and Gull, K. (1989). Definition of individual components within the cytoskeleton of Trypanosoma brucei by a library of monoclonal antibodies. *J. Cell Sci.* **93**, 491-500.

Wu, J. Q., McCormick, C. D. and Pollard, T. D. (2008). Chapter 9: Counting proteins in living cells by quantitative fluorescence microscopy with internal standards. *Methods Cell Biol.* **89**, 253-273.

Yan, H. and Balasubramanian, M. K. (2012). Meiotic actin rings are essential for proper sporulation in fission yeast. *J. Cell Sci.* **125**, 1429-1439.

Yan, H., Ge, W., Chew, T. G., Chow, J. Y., McCollum, D., Neiman, A. M. and Balasubramanian, M. K. (2008). The meiosis-specific Sid2p-related protein Slk1p regulates forespore membrane assembly in fission yeast. *Mol. Biol. Cell* **19**, 3676-3690.